

Inhibition of cytosolic and mitochondrial creatine kinase by siRNA in HaCaT- and HeLaS3-cells affects cell viability and mitochondrial morphology

Holger Lenz · Melanie Schmidt · Vivienne Welge · Thomas Kueper · Uwe Schlattner · Theo Wallimann · Hans-Peter Elsässer · Klaus-Peter Wittern · Horst Wenck · Franz Staeb · Thomas Blatt

Received: 22 May 2007 / Accepted: 12 July 2007 / Published online: 28 July 2007
© Springer Science+Business Media, LLC 2007

Abstract The creatine kinase (CK) system is essential for cellular energetics in tissues or cells with high and fluctuating energy requirements. Creatine itself is known to protect cells from stress-induced injury. By using an siRNA approach to silence the CK isoenzymes in human keratinocyte HaCaT cells, expressing low levels of cytoplasmic CK and high levels of mitochondrial CK, as well as HeLa cancer cells, expressing high levels of cytoplasmic CK and low levels of mitochondrial CK, we successfully lowered the respective CK expression levels and studied the effects of either abolishing cytosolic brain-type BB-CK or ubiquitous mitochondrial uMi-CK in these cells. In both cell lines, targeting the dominant CK isoform by the respective siRNAs had the strongest effect on overall CK activity. However, irrespective of the expression level in both cell lines, inhibition of the mitochondrial CK isoform generally caused the strongest decline in cell viability and cell proliferation. These findings are congruent with electron microscopic data showing substantial alteration of

mitochondrial morphology as well as mitochondrial membrane topology after targeting uMi-CK in both cell lines. Only for the rate of apoptosis, it was the least expressed CK present in each of the cell lines whose inhibition led to the highest proportion of apoptotic cells, i.e., downregulation of uMi-CK in case of HeLaS3 and BB-CK in case of HaCaT cells. We conclude from these data that a major phenotype is linked to reduction of mitochondrial CK alone or in combination with cytosolic CK, and that this effect is independent of the relative expression levels of Mi-CK in the cell type considered. The mitochondrial CK isoform appears to play the most crucial role in maintaining cell viability by stabilizing contact sites between inner and outer mitochondrial membranes and maintaining local metabolite channeling, thus avoiding transition pore opening which eventually results in activation of caspase cell-death pathways.

Keywords Creatine · Creatine kinase · siRNA · Mitochondria

H. Lenz (✉) · M. Schmidt · V. Welge · T. Kueper · K.-P. Wittern · H. Wenck · F. Staeb · T. Blatt
R&D, Beiersdorf AG, Unnastrasse 48, 20245 Hamburg, Germany
e-mail: holger.lenz@beiersdorf.com

T. Wallimann
Institute of Cell Biology, Swiss Federal Institute of Technology (ETH Zurich), Hoengergerberg HPM, Zurich 8093, Switzerland

U. Schlattner
INSERM, U884, Laboratory of Fundamental and Applied Bioenergetics, University Joseph Fourier, Grenoble, France

H.-P. Elsässer
Department of Cytobiology and Cytopathology, Philipps University Marburg, Robert-Koch-Str. 6, 35037 Marburg, Germany

Introduction

Creatine kinase (CK) forms a small family of isoenzymes playing an important role in maintaining the global and local ATP/ADP ratio at a constant high level within cells. With its substrates creatine (Cr) and phosphocreatine (PCr), CK isoenzymes provide a temporal and spatial cellular energy buffer. The reversible CK reaction, together with high concentrations of PCr, is able to replenish ATP levels for short-term peak energy requirements of cells, which cannot be replenished in time by conventional ATP generating pathways such as glycolysis or oxidative phosphorylation in mitochondria [1]. Further, the distinct

subcellular localizations of CK isoenzymes are thought to represent a PCr circuit, whereby sites of energy production (mitochondria and glycolysis) are tightly linked via highly diffusible Cr/PCr to sites of energy consumption [2]. ATP generated, e.g., by oxidative phosphorylation is used by mitochondrial CK (Mi-CK) to generate PCr from Cr [3, 4]. PCr then diffuses to the cytosol to locally regenerate ATP from ADP via cytosolic CK that is partially associated with cellular ATPases. Cr produced during this reaction is shuttled back to the mitochondria for recharging to PCr. This energy shuttling system is particularly efficient in tissues with a very high and fluctuating energy demand such as skeletal and cardiac muscle. However, it is also found in brain, kidney, uterus, spermatozoa, and most other cells and tissues investigated so far [5–7], including skin [8, 9], indicating an important role in cellular energy homeostasis.

Recent experiments with Cr supplementation *in vitro* and *in vivo* show that not only CK but also its substrates Cr and PCr are important for proper cell function. The best line of evidence for this comes from the recent discovery of the so-called Cr-deficiency syndromes involving patients that lack Cr in their brain and present with a severe phenotype (for review see [10]). *In vitro* treatment of cells, as well as dietary supplementation of animals with Cr can improve the cellular stress resistance in general, enhance survival following noxious treatment and protect from injury [11, 12]. Cr supplementation mediates remarkable neuroprotection in experimental models of several neurodegenerative diseases [13–15], as well as traumatic brain injury [12], and cerebral ischemia in mice [16]. Transgenic mice expressing high levels of BB-CK in liver cells, which are normally devoid of this enzyme, become more resistant to apoptosis induced by tumor necrosis factor or hypoxia when supplemented with dietary Cr [17]. Furthermore, our own data demonstrate that Cr exhibits a protective effect against oxidative stress in skin, caused by reactive oxygen species (ROS) [9]. Such protective effects of Cr may be linked to an increased cellular PCr pool [18], which would improve the energy buffer and storage functions of the CK system. In conjunction with Mi-CK, Cr shows a number of additional beneficial effects, either in preventing apoptosis by inhibiting mitochondrial permeability transition [3, 19], or in controlling production of noxious ROS [20] by tight functional coupling of Mi-CK to oxidative phosphorylation [21]. These mechanisms would improve the stress resistance of cells by preventing a drop in ATP/ADP ratios, premature apoptosis, and/or ROS-induced cellular damage.

In an attempt to elucidate the functional role of CK isoenzymes *in vivo*, constitutive knockout mice lacking cytosolic and/or mitochondrial CK were generated and studied extensively [22–30]. Although the mice were phenotypically normal in many aspects, detailed

characterization revealed a number of impairments. While single CK knockouts showed some histological and biochemical adaptations or abnormal behavior [26, 27], the phenotypes of double knockouts were much more pronounced, including severely impaired calcium handling in muscle [23, 31], spatial learning [29], and hearing loss [7]. Two conclusions could be drawn from these studies. First, the existence of a functional Cr/PCr system is very important, although not absolutely mandatory for survival. Second, constitutive CK gene knockout mice develop a remarkable metabolic and morphological remodeling of their cells and tissues to compensate for the lack of CK, thus possibly obscuring the primary phenotype linked to the gene knockout [22–30].

Therefore, the aim of this study was to adopt an siRNA approach to silence CK isoenzymes on a fast time scale and thus prevent compensatory adaptations. Using human keratinocyte HaCaT and cancer HeLa cells, that express different levels of BB-CK and uMi-CK, we successfully lowered CK expression levels of both isoenzymes and studied the effects on cell viability and ultrastructure. Our results provide new insight into the role of cytoplasmic versus mitochondrial CK in providing stress resistance. Notably, a strong mitochondrial phenotype was observed in uMi-CK siRNA targeted cells, showing altered mitochondrial morphology as well as mitochondrial membrane topology, a finding that is in line with the proposed function of uMi-CK in stabilizing contact sites between inner and outer mitochondrial membranes [32] and in reducing ROS-mediated damage [20]. In contrast to the transgenic CK knockout animal models, siRNA silencing of CK seems to impose a more severe phenotype affecting cell viability and survival, possibly due to the lack of compensatory metabolic and morphological adaptations in this experimental model.

Materials and methods

Cell culture

The human keratinocyte cell line HaCaT, and HeLaS3, cells were cultured at 37°C and 7% CO₂ in 185 cm² culture flasks (Nunc, Wiesbaden, Germany) containing Dulbecco's modified Eagle's medium (Life Technologies, Eggenstein, Germany) supplemented with 10% fetal calf serum (Life Technologies, Eggenstein, Germany). Medium was replaced twice weekly. After cells reached a confluency of 50–70%, cells were split 1:4 or seeded in 6 well plates (10,000 cells/cm²). After an additional 24 h of incubation, the cells were used for the experiments described below.

Table 1 siRNA sequences used for inhibition of human BB-CK and uMi-CK expression

siBB-CK:	5'-CCU GGG CAA GCA UGA GAA G dTdT (G/C content: 54.4%)
siMi-CK:	5'-UGA AGC ACA CCA CGG AUC U dTdT (G/C content: 47.6%)

siRNA against BB-CK starts at basepair 900 of the coding sequence and siRNA against uMi-CK at basepair 786. G/C content: ratio of guanine and cytosine nucleic acids in total siRNA sequence

Transfection with siRNAs

The transfection was performed using Lipofectamine PlusTM (Invitrogen, Karlsruhe, Germany). In brief, 10 μ l of Scramble, siBB-CK, or siMi-CK siRNAs (20 μ M, MWG Biotech, Munich, Germany) were premixed with 86 μ l medium (Dulbecco's modified Eagle's medium, Life Technologies, Eggenstein, Germany) and 4 μ l Plus-solution in a 1.5 ml-test tube. The siRNA sequences used for inhibition of human BB-CK and Mi-CK expression are depicted in Table 1. Lipofectamine (4 μ l) was premixed in 96 μ l medium in another 1.5 ml-test tube. After 10 min of incubation, solutions from both test tubes were mixed and incubated for another 15–20 min. In the meantime, the medium from the 6 well plates containing HaCaT- or HeLaS3- cells was removed, cell layers were rinsed with PBS, and 800 μ l serum-free medium was added to each well. The 200 μ l transfection mixture was added to each well and carefully mixed. Transfection was stopped 24 h later by adding 500 μ l medium containing 30% fetal calf serum.

Cell extracts

Cells, seeded and incubated in 6-well plates, were washed twice with ice-cold PBS. Afterwards 200 μ l lysis buffer (50 mM Tris-HCl, 5 mM EDTA, 300 mM NaCl, 0.5% Triton X 100), containing CompleteTM Mini (Roche) protease inhibitor cocktail, were added to each well and incubated for 30 min at room temperature. After scraping the cells, the suspension was centrifuged for 10 min at 14,000 rpm and 4°C. The protein amount was determined by using a BCA assay (Interchim, Montiucon, France) and the absorption at 562 nm was measured in 96-well plates on a Spectra Max 250 (Molecular Devices, Sunnyvale, USA).

Antibodies and immunoblotting

Proteins from cell extracts (10 μ g per lane) were separated by polyacrylamide gel electrophoresis under denaturing conditions on 10% SDS-PAGE gels. Subsequently, the proteins were electrotransferred onto nitrocellulose or

PVDF membranes and blocked with 10 % milk powder. CK isoenzymes were identified using a rabbit-anti-human BB-CK primary antibody (Biotrend, Köln, Germany) or a rabbit-anti-human uMi-CK primary antibody [8], followed by secondary anti-rabbit IgG antibodies conjugated to horseradish peroxidase (Sigma, Munich, Germany). The protein bands were visualized using the Lumilight Plus Western Blot Detection Kit (Roche, Mannheim, Germany).

Determination of CK activity

Cytoplasmic extracts (10 μ l) of siRNA-transfected and control cells were used in a CK assay (Sigma, Munich, Germany) as described before [9]. In brief, Cr solution (50 μ l) was added to one sample of each cytoplasmic extract (test), and 50 μ l TRIZMA buffer was added to another sample (blank). In the following steps the samples were all treated analogously. After addition of 50 μ l water and 5 min incubation at 37°C, 4 μ l ATP-glutathione was added and the samples were incubated at 37°C for 1 h. The reaction was then stopped with 80 μ l of 20% trichloroacetic acid (TCA) and filtered through a multiscreen plate (Millipore). After addition of 200 μ l water, 50 μ l acid molybdate, and 12.5 μ l Fisk & Subarow reducer to 50 μ l of each sample, they were incubated at room temperature for 30 min. Finally, the absorbance at 700 nm was measured, the amount of phosphate (in μ g) was determined according to a standard curve, and the difference (Δ μ g phosphate) between blank and test were transformed into CK activity units.

Determination of vitality (lactate dehydrogenase release)

Cell vitality was determined using the Cytotoxicity Detection Kit (LDH, Roche, Mannheim, Germany). The assay is based on the cleavage of a tetrazolium salt when LDH is present in the culture supernatant. In brief, HaCaT, and HeLaS3 cells were seeded in 6 well plates at 100,000 cells/well and cultured for 24 h before transfection with Scramble, siBB-CK, or siMi-CK siRNAs. Cytotoxicity in both cell lines was measured 72 h after transfection. Lactate dehydrogenase activity was determined in 100 μ l aliquots of the 1.5 ml-culture supernatant and in 100 μ l aliquots of the corresponding 1.5 ml-lysate of the remaining cells (lysis in 2% Triton-X 100 for 10 min). For colorimetric determination of LDH, 100 μ l of either the culture supernatants or the lysates were combined with 100 μ l of the test reagent on 96-well ELISA microplates and incubated for 30 min at room temperature. Absorbance was measured at 492 nm using an ELISA plate reader (Spectramax, Molecular Devices, Munich,

Germany). Cytotoxicity was expressed as the ratio of released LDH activity in supernatants and total LDH activity.

Determination of cell proliferation (BrdU incorporation)

Proliferation in HaCaT- and HeLaS3-cells was measured 72 h after transfection with Scramble, siBB-CK or siMi-CK by determination of BrdU incorporation using the Proliferation-ELISA BrdU (Roche, Mannheim, Germany). The Proliferation ELISA measures cell proliferation by quantitation of BrdU incorporated into newly synthesized DNA of replicating cells. In brief, HaCaT- and HeLaS3-cells were seeded in 6 well plates at 100,000 cells/well and cultured for 24 h before transfection with Scramble, siBB-CK, or siMi-CK siRNAs. Cells were then incubated for 24 h with BrdU starting 48 h after transfection. The cells were subsequently fixed with FixDenat solution for 30 min, followed by incubation with 1.5 ml of the anti-BrdU-POD-solution for 90 min. After three washes TMB substrate solution was added for 30 min, and the resulting absorbance at 370 nm (reference wavelength 492 nm) was determined by means of an ELISA plate reader (Spectramax, Molecular Devices, Munich, Germany).

Determination of apoptosis and necrosis (FACS)

Apoptosis and necrosis were determined using the Annexin V-FITC Apoptosis detection Kit I (BD Biosciences, Heidelberg, Germany). In brief, HaCaT- and HeLaS3-cells were detached 72 h after transfection from the culture plates using Trypsin/EDTA buffer (10 min at 37°C). Harvested cells were washed twice with cold PBS and resuspended in 100 µl binding buffer. Fifteen minutes after adding 5 µl annexin-V-FITC and 5 µl propidium iodide (PI) the cell suspension was diluted to 500 µl with binding buffer and analyzed with a FACScalibur flow cytometer (Becton Dickinson, Heidelberg, Germany) using a two-color setting. Viable cells were identified as annexin-V negative and PI negative cells; apoptotic cells as annexin-V positive and PI negative, necrotic cells as annexin-V positive and PI positive.

Electron microscopy

HaCaT- and HeLaS3-cells were washed 72 h after transfection with ice-cold PBS without Ca²⁺ and Mg²⁺ (PAA, Linz, Austria) and incubated at 4°C in 1 ml of a 1:1 mixture of freshly prepared fixative according to Ito and Karnovsky [33] (5 ml of 5% paraformaldehyd in 0.2 M cacodylate buffer, 1 ml 25% glutaraldehyde, 3 ml water, 1 ml 0.5% picric acid) and cacodylate buffer (0.2 M sodium cacodylate, pH 7.35) for 1 h (all chemicals from

Sigma, Munich, Germany). After centrifugation at 1500 rpm for 10 min in a 1.5 ml test-tube, cells were washed four times with 1 ml 0.1 M cacodylate buffer for 10 min and spun at 1500 rpm for 10 min. Afterwards, cells were incubated with 1 ml of osmium fixation solution (1:1 mixture of 2% osmium tetroxide and 3% potassium ferricyanate, both Sigma, Munich, Germany) for 1 h and washed with water several times. The fixed tissue was embedded in Epon resin according to standard procedures, cut on a Ultracut FC 4E microtome (Reichert-Jung, Nussloch, Germany) and finally microscopied on a Zeiss EM109 electron microscope (Zeiss, Göttingen, Germany) using a Macophot ORT25c film (G.C.Bender, Frankfurt, Germany).

Results

Creatine kinase expression in HaCaT- and HeLaS3-cells

A representative Western blot analysis of cytoplasmic BB-CK and mitochondrial uMi-CK in lysates of keratinocytes, HaCaT- and HeLaS3-cells is shown in Fig. 1. Isoform-specific antibodies detected both CK isoenzymes as distinct bands with an apparent molecular weight of about 43 kDa. BB-CK and uMi-CK were differentially expressed in HaCaT- and HeLaS3-cells: while HaCaT cells and keratinocytes showed low BB-CK and high uMi-CK levels, the opposite was the case for HeLaS3-cells, with high BB-CK and particularly low uMi-CK levels.

Inhibition of BB-CK and uMi-CK in HaCaT- and HeLaS3-cells by siRNA

For inhibition of BB-CK and uMi-CK in HaCaT- and HeLaS3-cells, isoform-specific siRNAs (siBB-CK and siMi-CK; Table 1) were chosen according to recommendations described by Elbashir et al [36]. A representative Western blot analysis of cell lysates from untransfected HaCaT- and HeLaS3-cells, as well as cells transfected with Scramble siRNA (not encoding for any known human target sequence), siBB-CK, siMi-CK, and a combination of siBB-CK and siMi-CK is depicted in Fig. 2. In both, HaCaT- and HeLaS3-cells transfection with Scramble siRNA did not show any effect on the expression of BB-CK or uMi-CK. As expected, transfection of both cell lines with siBB-CK (Fig. 2A, C) clearly inhibited BB-CK expression by about 75% (HaCaT) and 92% (HeLaS3). Transfection with siMi-CK (Fig. 2B) also reduced uMi-CK expression by about 80% in HaCaT-cells, while in HeLaS3-cells with their very low uMi-CK levels (Fig. 1B), an inhibition of this isoenzyme was not detectable (not

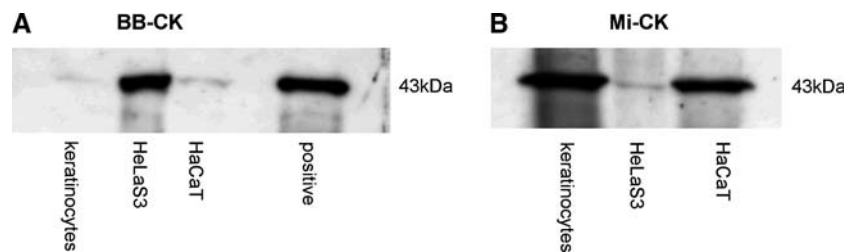


Fig. 1 CK expression and activity in HaCaT- or HeLaS3-cells. Western blot analysis of BB-CK (**A**) and uMi-CK (**B**). Cytosolic extracts (10 μ g of total protein) of human primary keratinocytes, HeLaS3 and HaCaT cells were separated by SDS-PAGE. Purified BB-CK (positive) served as a positive control in A. As negative control, the primary antibody was omitted (data not shown).

shown). However, it is important to note that siBB-CK had no effect on uMi-CK expression, while siMi-CK also inhibited expression of BB-CK by about 75%, almost similar to a mixture of both siRNAs as seen with HaCaT cells (Fig. 2A, C). In the following assays, effects of CK down-regulation were determined 72 h after transfection.

Effects of CK siRNA inhibition on CK activity

The effect of siRNAs on CK expression was also detected by measuring overall CK activity. Cells transfected with siBB-CK or siMi-CK were compared to those transfected with Scramble control (Table 2). Overall CK activity in HaCaT-cells was unaffected by siBB-CK, but significantly reduced ($P = 0.041$) by siMi-CK. The inverse was true for HeLaS3-cells, where siBB-CK led to a highly significant ($P = 0.014$) reduction of overall CK activity, while changes in siMi-CK levels were not significant. These results coincide with the different abundance of CK isoenzymes in these cell lines: high levels of uMi-CK in HaCaT, but high levels of cytoplasmic BB-CK in HeLaS3 (Fig. 1).

Effects of BB-CK and Mi-CK siRNA inhibition on cell viability

The effect of reduced BB-CK and uMi-CK levels on cell viability and proliferation was examined in HaCaT and HeLaS3-cells. First, the rate of cell death was determined by measuring lactate-dehydrogenase-(LDH)-release into the supernatant of siRNA-transfected cells (Table 3). In HaCaT cells, transfection with siBB-CK had no effect at all, and transfection with siMi-CK led to an only weak increase ($P = 0.057$) in the rate of cell death as normalized to Scramble control. By contrast, transfection of HeLaS3-cells with both, siBB-CK and siMi-CK, showed a highly significant ($P = 0.013$ and $P = 0.003$, respectively) increase in the rate of cell death. Here, the strong effect of siMi-CK is probably due to inhibition of both, uMi-CK and BB-CK expression (Fig. 2C).

Molecular weight (about 43 kDa for BB-CK and uMi-CK) was determined by using a molecular weight standard (Precision Plus, dual color) from Bio-Rad (Munich, Germany). The Western blots were repeated three times and representative blots were chosen for this figure

As a second parameter, proliferation was examined using a BrdU incorporation assay (Table 4). Transfection with siRNA against BB-CK had only little effects on proliferation of HaCaT- and HeLaS3-cells, whereas transfection with siMi-CK showed a highly significant reduction ($P = 0.018$ and $P = 0.024$, respectively) of proliferation in HaCaT-cells and HeLaS3-cells as well. Since siBB-CK is inefficient in this assay, the strong effect of siMi-CK is rather due to reduced uMi-CK levels. This is surprising for HeLa cells, which express only low levels of this isoenzyme (Fig. 1).

As a third parameter, percentages of apoptotic and necrotic cells after siRNA transfection of HaCaT- and HeLaS3-cells were determined by FACS analysis using PI and annexin-V-FITC for labeling. Compared to Scramble control, a shift from vital to apoptotic and necrotic cells could be observed in all transfections (Table 5). In HaCaT-cells, transfection with siBB-CK showed the strongest effects with an increase of apoptotic (by 19%) and necrotic cells (by 10%). Transfection with siMi-CK only slightly increased the rate of apoptotic (by 6%) and necrotic cells (by 7%). In contrast, transfection of HeLaS3-cells with siBB-CK showed less increase in apoptotic (by 25%) and necrotic cells (by 7%) than transfection with siMi-CK. In the latter case, apoptosis rose by 37% and necrosis by 15%, leaving only about 14% of cells in the vital state.

Effects of BB-CK and Mi-CK siRNA inhibition on cell morphology

The effects of transfection with siBB-CK and siMi-CK on the morphology of HaCaT- and HeLaS3-cells were examined by transmission electron microscopy (Fig. 3). Neither in HaCaT- nor in HeLaS3-cells, morphological changes could be detected after transfection with siBB-CK (data not shown). In contrast, inhibition of Mi-CK (together with BB-CK) using siMi-CK had visible effects on cellular morphology of both cell types. As compared with untransfected (Fig. 3A + D) and Scramble-transfected cells

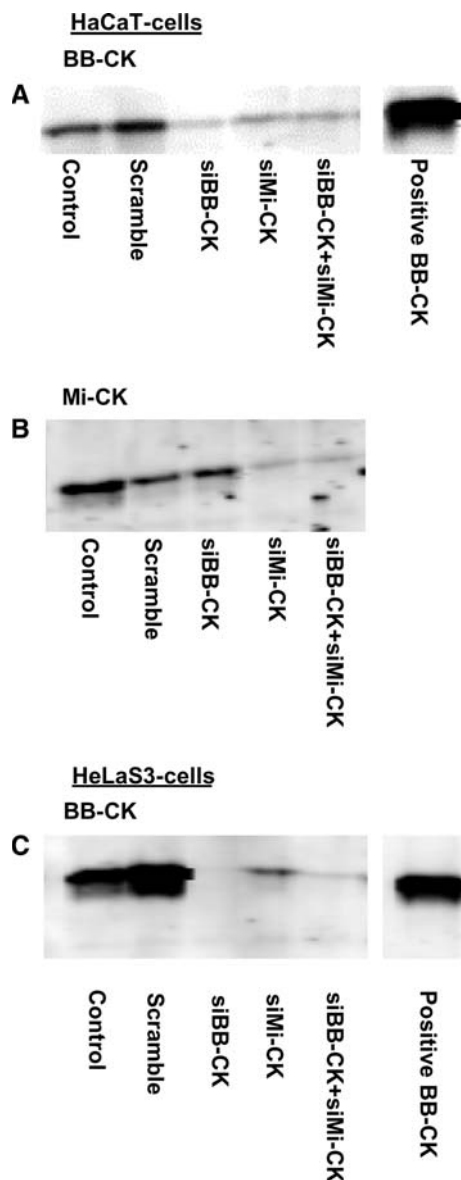


Fig. 2 Transfection of HaCaT- and HeLaS3-cells with siBB-CK or siMi-CK. Western blot analysis of BB-CK (A and C) and Mi-CK (B) after transfection of HaCaT-cells (A and B) and HeLaS3-cells (C) with siBB-CK or siMi-CK. For Western blot analysis cytosolic extracts of HaCaT- and HeLaS3-cells (10 μ g of total protein) were prepared and separated by SDS-PAGE. Untreated cells (Control), Scramble treated, siBB-CK or siMi-CK treated cells were compared. Purified BB-CK (positive) served as a positive control in A and C. As negative control, the primary antibody was omitted (data not shown). Molecular weights were determined by using a molecular weight standard (Precision Plus, dual color) from Bio-Rad (Munich, Germany). The Western blots were repeated three times and representative blots were chosen for this figure

(Fig. 3B + E), siMi-CK transfected cells showed mitochondria with a significantly altered ultrastructure and cristae disposition (Fig. 3C + F). This morphology coincided with a decrease in mitochondrial membrane potential

Table 2 CK activity after transfection of HaCaT- and HeLaS3-cells with siRNAs against BB-CK or uMi-CK

	CK activity after transfection (% of Scramble control)		
	Scramble	siBB-CK	siMi-CK
HaCaT	100 \pm 16	117 \pm 23	38 \pm 24*
HeLaS3	100 \pm 43	21 \pm 27**	51 \pm 39

Creative kinase activity was measured in cytosolic extracts of HaCaT- and HeLaS3-cells 72 h after transfection with Scramble, siBB-CK and siMi-CK. All data represent the mean \pm SD of triplicate measurements and were normalized to the scramble control (100%). No differences were observed between untransfected and Scramble-transfected cells (not shown)

* P < 0.05 as compared with Scramble control; ** P < 0.025 as compared with Scramble control

Table 3 Cytotoxicity (LDH release) after transfection of HaCaT- and HeLaS3-cells with siRNAs against BB-CK or uMi-CK

	LDH release after transfection (% of Scramble control)		
	Scramble	siBB-CK	siMi-CK
HaCaT	100 \pm 19	108 \pm 5	129 \pm 5*
HeLaS3	100 \pm 6	165 \pm 35**	217 \pm 41**

Cytotoxicity in HaCaT- and HeLaS3-cells was determined by LDH release measurement 72 h after transfection with Scramble, siBB-CK or siMi-CK by determination of LDH activity. All data represent the ratio of LDH release into the media versus total LDH. Data represent means \pm SD of five measurements and were normalized on Scramble control (100 %). No differences were observed between untransfected and Scramble-transfected cells (not shown)

* P = 0.057 as compared with Scramble control; ** P < 0.025 as compared with Scramble control

Table 4 Proliferation (BrdU incorporation) after transfection of HaCaT- and HeLaS3-cells with siRNAs against BB-CK or uMi-CK

	BrdU incorporation after transfection (% of Scramble control)		
	Scramble	siBB-CK	siMi-CK
HaCaT	100 \pm 11	81 \pm 11	56 \pm 1*
HeLaS3	100 \pm 21	83 \pm 1	43 \pm 16*

Proliferation in HaCaT- and HeLaS3-cells was measured 72 h after transfection with Scramble, siBB-CK or siMi-CK by BrdU incorporation for 24 h. All data represent means \pm SD of triplicate cultures and were normalized to the Scramble control (100%). No differences were observed between untransfected and Scramble-transfected cells (not shown)

* P < 0.025 as compared with Scramble control

(data not shown). Moreover, the storage glycogen observed in untransfected and Scramble control HeLaS3-cells (Fig. 3D + E) vanished nearly completely in siMi-CK transfected HeLaS3-cells (Fig. 3F).

Table 5 Apoptosis and necrosis after transfection of HaCaT- and HeLaS3-cells with siRNAs

Cell line	Transfection	Cellular status 72 h after transfection		
		Vital (%)	Apoptotic (%)	Necrotic (%)
HaCaT	Scramble	75.6	21.0	3.4
HaCaT	siBB-CK	46.8	40.0	13.2
HaCaT	siMi-CK	63.1	26.9	10.1
HeLaS3	Scramble	65.3	32.2	2.4
HeLaS3	siBB-CK	33.1	57.6	9.2
HeLaS3	siMi-CK	13.9	69.0	17.1

Percentages of vital cells (annexin-V⁻/PI⁻), apoptotic cells (annexin-V⁺/PI⁻), and necrotic cells (annexin-V⁺/PI⁺) were determined 72 h after transfection with Scramble, siBB-CK and siMi-CK by FACS analysis using Annexin V and propidium iodide (PI) staining. Data represent means of triplicate measurements. No differences were observed between untransfected and Scramble-transfected cells (not shown)

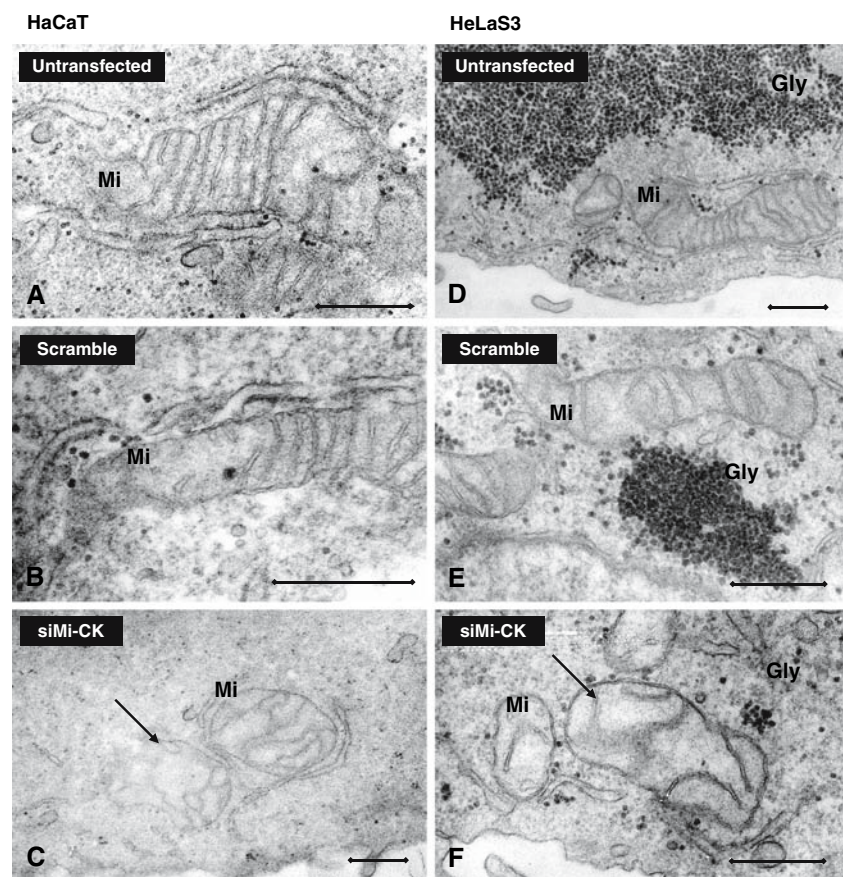
Discussion

In this article, we first describe the effects of selective siRNA inhibition of cytosolic and mitochondrial CK in cell culture with regard to cell viability and morphology. The data suggest that a major phenotype is linked to reduction

of mitochondrial CK alone or in combination with cytosolic CK, and that this effect is independent of the relative expression levels of Mi-CK in the cell type considered. Thus, immediate down-regulation of CK in cell culture leads to a more severe phenotype as compared to constitutive CK knockout mice.

Here we used two human cell lines, keratinocyte HaCaT-cells and cervical carcinogenic HeLaS3-cells for which we show an inverse CK expression pattern: low levels of cytoplasmic BB-CK and high levels of mitochondrial uMi-CK in HaCaT-cells, but high levels of BB-CK and low levels of uMi-CK in HeLaS3-cells. Both CK isoenzymes were successfully down-regulated by a targeted siRNA. This approach has not yet been used to manipulate CK expression and can complement the large number of studies on constitutive CK knockdown mice [22–30, 34]. The cell phenotype was examined 72 h after transfection. This should eliminate most metabolic and cyto-architectural adaptations which complicate analysis of the classical constitutive mouse knockdown models [23–25], and thus facilitate detection of primary consequences of CK inhibition. In addition, the opposite CK expression pattern of the two cell lines gave us the opportunity to distinguish between the different effects of inhibition of either cytosolic or mitochondrial CK. Expression levels of

Fig. 3 Transmission electron microscopy after transfection of HaCaT- and HeLaS3- cells with siRNA against Mi-CK. Transmission electron microscopy images of HaCaT- (A, B, C) and HeLaS3- (D, E, F) cells 72 h after transfection with siRNA. A and D represent non-transfected control cells, B and E scramble control cells and C and F cells transfected with siMi-CK. Note that the ultrastructure and cristae disposition in the mitochondria of siMi-CK transfected HaCaT- and HeLaS3-cells is significantly altered. The scale bar corresponds to 0.5 μ m. Mi: mitochondria, Gly: glycogen, arrow: chistae



BB-CK and uMi-CK were generally down-regulated by 75% or more. While siBB-CK was specific for BB-CK, transfection with siMi-CK affected not only uMiCK but also BB-CK levels. This unexpected result was observed at the protein level for both cell types, and also with total CK enzyme activity in case of HeLaS3-cells, where siMi-CK provokes a marked CK activity decrease, although uMi-CK is present at only marginal amounts. A reason for this observation could be an unexpected cross-reactivity of the chosen siMi-CK RNA, although its sequence is specific for uMi-CK (see Table 1) and was the most efficient among several tested ones. Theoretically, siMi-CK could also reduce BB-CK expression indirectly, secondary to uMt-CK inhibition, but this was not observed in transgenic mice carrying an invalidated uMt-CK gene [29].

The effects of CK down-regulation on viability and morphology of both cell lines are summarized in Table 6. These are the two parameters that are frequently altered in experimental models of Cr supplementation or CK knockdown. In the present study, using siRNA-induced acute down-regulation of BB-CK or uMi-CK, rather different and pronounced phenotypes were observed. They can be grouped in those that are largely determined by inhibition of Mi-CK, and others that seem to be more cell-type specific.

In both cell lines, siMi-CK led to a distinct strong reduction in cell proliferation, increased necrosis, drastic changes in mitochondrial shape and morphology, as well as in HeLaS3-cells to a strong reduction in storage glycogen. The siBB-CK had very weak or no effect on these

parameters, indicating that it is rather uMi-CK inhibition that is at the basis of the distinct siMi-CK effects. The close link between CK and proliferation as an energy-dependent process has been reported frequently, in particular in oncogenic growth [35]. However, this mostly concerned cytosolic BB-CK, while our results suggest an important role rather for Mi-CK. Mitochondrial morphology in siMi-CK transfected cells could be directly observed by electron microscopy, revealing an alteration in the global morphological appearance of mitochondria from elongated to more spherical organelles, and a loss of normal cristae membrane topology showing fewer cristae with enlarged cristae space.

Together with a reduced membrane potential (data not shown), these data indicate a partial loss of function of the mitochondrial compartment as a consequence of uMi-CK inhibition, regardless whether this is the predominantly expressed isoenzyme or present only in faint amounts like in HeLaS3-cells. This finding has two important implications.

First, it corroborates the already known specific roles of Mi-CK in maintaining coupled ATP-ADP exchange across the inner membrane [21], minimizing ROS generation [20], and stabilizing the mitochondrial inner and outer membranes at contact sites [32]. As a consequence, functional MtCK together with its substrate Cr not only supplies an energy buffer and transport system, but may also help to protect mitochondria from membrane damage and opening of the permeability transition pore [3, 36], an early event of apoptosis [37]. Immediate and strong downregulation of Mi-CK seems to interfere with all these functions, leading

Table 6 Summary of CK isoenzyme expression and effects of siRNA transfection in HaCaT- and HeLaS3-cells

	HaCaT-cells		HeLaS3-cells	
	BB-CK	uMiCK	BB-CK	uMiCK
CK isoenzyme:	BB-CK	uMiCK	BB-CK	uMiCK
Expression	Low	High	High	Low
Transfection with siRNA	siBB-CK	siMi-CK	siBB-CK	siMi-CK
<i>Cell physiological parameters</i>				
CK-activity	o	–	– –	(–)
Cytotoxicity (LDH)	o	(+)	++	++
Proliferation (BrdU)	o	– –	o	– –
Apoptosis	(+)	(+)	(+)	(+)
Necrosis	(+)	(+)	(+)	+ +
<i>Cell morphological parameters</i>				
Mitochondrial ultrastructure	Unchanged	Changed	Unchanged	Changed

The different effects of siRNA transfection on HaCaT- and HeLaS3-cells with siRNAs against cytosolic BB-CK and mitochondrial uMi-CK are summarized in comparison with the observed endogenous expression levels of the two different CK isoforms. Cell physiological parameters were determined 72 h after transfection

++/– – Statistically highly significant stimulation/inhibition ($P < 0.025$)

+/- Statistically significant stimulation/inhibition ($P < 0.05$)

o No difference

(+)(-) Tendency toward stimulation/inhibition

to apoptotic or necrotic cell death. The latter is seen mainly in HeLa cells, probably because mitochondria are strongly impaired and cellular ATP levels are too low.

Second, the phenotype of the siRNA model seems to be much more severe than with CK knockout mice, in particular those with both CK isoenzymes invalidated [23, 25]. As already mentioned, this is probably due to the multiple compensatory adaptations in these animals. For example, proliferation of functional mitochondria was observed that could compensate ATP generation and diffusion limitations due to loss-of-function in the Cr/PCr system. Furthermore, MM-CK and MM-CK/sMi-CK double knockouts showed a compensatory increase in glycogen content in fast muscle fibers [23], while in our experiments siMi-CK led to a strong decrease of storage glycogen in HeLa cells, possibly as a consequence of energy stress. Together with further metabolic remodeling, these adaptations of CK knockout animals are apparently sufficient to avoid dramatic energy loss and to prevent premature cell death, in contrast to what was observed in the siRNA model. Taken together, these data suggest that the phenotype of CK knockout animals is obscured by a number of secondary adaptations of the metabolic network.

Other effects of CK down-regulation seemed to be rather cell-type specific and dependent on the different isoenzyme expression pattern. HaCaT-cells were almost resistant to cytotoxicity induced by CK down-regulation; only inhibition of the major uMi-CK isoenzyme showed an effect at low significance. Strong cytotoxicity was detected in HeLaS3-cells for both siRNAs. However, the strong effect of siMi-CK is here rather due to BB-CK down-regulation, since already siBB-CK shows a strong phenotype. For induced apoptosis, again HeLaS3-cells were the more susceptible. Interestingly, here it was the least expressed CK present in each of the cell lines whose inhibition led to the highest proportion of apoptotic cells, i.e., downregulation of Mi-CK in case of HeLaS3. Thus, there seems to be a direct correlation between uMi-CK expression level and apoptosis in this cell line.

Creatine kinase is a key enzyme for cellular energetics in tissues or cells with high and fluctuating energy requirement, such as skeletal, cardiac and smooth muscle, as well as brain, retina photoreceptor cells, spermatozoa, and inner ear sensory hair cells [4, 6, 7, 38]. Cr itself is known for numerous beneficial effects in muscle, such as increasing muscle strength and endurance [18, 39–43]. Moreover it has neuroprotective properties in neurodegenerative diseases like Parkinson or amyotrophic lateral sclerosis [13, 44–46] or traumatic brain [12] and spinal cord [47] injury. It prevents of mutagenesis of mitochondrial DNA [48] and has protective effects against UV damage in skin [9, 48], just to mention a few of the effects that were observed in various systems.

Data obtained with siRNA technology in this study shed new light on the importance of CK isoforms for normal cell function in keratinocytes and thus in skin, as well as in cancer. They corroborate the relevance of CK [8] and its substrates Cr and PCr for skin function, maintenance, protection [9], and repair [49]. In particular, the data support findings that Mi-CK plays a number of specific structural and functional roles, even if present only as a minor isoenzyme. These functions include stabilization of specific contact sites linking inner and outer mitochondrial membranes [32], reduction of ROS generation [20], and inhibition of mitochondrial permeability transition [3, 36], an early event of apoptosis [37]. The study represents a proof of principle for siRNA inhibition of CK. This technology seems to be a valuable tool to examine the multifaceted role of CK isoenzymes in the complex cellular metabolic networks.

Acknowledgments We thank Dr. Gesa Muhr and Dr. Ute Breitenbach, Beiersdorf AG (Hamburg, Germany) for support of the siRNA transfection experiments. Further we thank Ursula Lehr, Brigitte Agricola, and Volkwin Kramer, Department of Cytobiology and Cytopathology (Philipps University, Marburg) for their assistance with the transmission electron microscopy and photography. This work was supported by a grant from the Swiss National Science Foundation No. 31000AO-102075 (to T.W. and U.S.) and a “Chaire d’excellence” (ANR France, to U.S.).

References

1. Wallimann T, Wyss M, Brdiczka D et al (1992) Intracellular compartmentation, structure and function of creatine kinase isoenzymes in tissues with high and fluctuating energy demands: the ‘phosphocreatine circuit’ for cellular energy homeostasis. *Biochem J* 281(Pt 1):21–40
2. Wallimann T, Tokarska-Schlattner M, Neumann D et al (2007) The phospho-creatine circuit: molecular and cellular physiology of creatine kinases sensitivity to free radicals and enhancement by creatine supplementation. In: Saks V (ed) *Molecular systems bioenergetics: basic principles, organization and dynamics of cellular energetics*. Wiley Publisher Co., USA
3. Dolder M, Walzel B, Speer O et al (2003) Inhibition of the mitochondrial permeability transition by creatine kinase substrates. Requirement for microcompartmentation. *J Biol Chem* 278:17760–17766
4. Schlattner U, Tokarska-Schlattner M, Wallimann T (2006) Mitochondrial creatine kinase in human health and disease. *Biochim Biophys Acta* 1762:164–180
5. Wallimann T, Hemmer W (1994) Creatine kinase in non-muscle tissues and cells. *Mol Cell Biochem* 133–134:193–220
6. Kaldis P, Kamp T, Piendl T et al (1997) Functions of creatine kinase isoenzymes in spermatozoa. *Adv Dev Biochem* 5:275–312
7. Shin JB, Streijger F, Beynon A et al (2007) Hair bundles are specialized for ATP delivery via creatine kinase. *Neuron* 53:371–386
8. Schlattner U, Mockli N, Speer O et al (2002) Creatine kinase and creatine transporter in normal, wounded, and diseased skin. *J Invest Dermatol* 118:416–423
9. Lenz H, Schmidt M, Welge V et al (2005) The Creatine kinase system in human skin: protective effects of creatine against

- oxidative and UV damage in vitro and in vivo. *J Invest Dermatol* 124(2):443–452
10. Schulze A (2003) Creatine deficiency syndromes. *Mol Cell Biochem* 244:143–150
 11. Brewer GJ, Wallimann TW (2000) Protective effect of the energy precursor creatine against toxicity of glutamate and beta-amyloid in rat hippocampal neurons. *J Neurochem* 74:1968–1978
 12. Sullivan PG, Geiger JD, Mattson MP et al (2000) Dietary supplement creatine protects against traumatic brain injury. *Ann Neurol* 48:723–729
 13. Klivenyi P, Ferrante RJ, Matthews RT et al (1999) Neuroprotective effects of creatine in a transgenic animal model of amyotrophic lateral sclerosis. *Nat Med* 5:347–350
 14. Matthews RT, Ferrante RJ, Klivenyi P et al (1999) Creatine and cyclocreatine attenuate MPTP neurotoxicity. *Exp Neurol* 157:142–149
 15. Ferrante RJ, Andreassen OA, Jenkins BG et al (2000) Neuroprotective effects of creatine in a transgenic mouse model of Huntington's disease. *J Neurosci* 20:4389–4397
 16. Zhu S, Li M, Figueroa BE et al (2004) Prophylactic creatine administration mediates neuroprotection in cerebral ischemia in mice. *J Neuroscience* 24:5909–5912
 17. Hatano E, Tanaka A, Kanazawa A et al (2004) Inhibition of tumor necrosis factor-induced apoptosis in transgenic mouse liver expressing creatine kinase. *Liver Int* 24:384–393
 18. Vandenberghe K, Goris M, Van Hecke P et al (1997) Long-term creatine intake is beneficial to muscle performance during resistance training. *J Appl Physiol* 83:2055–2063
 19. Beutner G, Ruck A, Riede B et al (1998) Complexes between porin, hexokinase, mitochondrial creatine kinase and adenylate translocator display properties of the permeability transition pore. Implication for regulation of permeability transition by the kinases. *Biochim Biophys Acta* 1368:7–18
 20. Meyer LE, Machado LB, Santiago AP et al (2006) Mitochondrial creatine kinase activity prevents reactive oxygen species generation: antioxidant role of mitochondrial kinase-dependent ADP re-cycling activity. *J Biol Chem* 281:37361–37371
 21. Kay L, Nicolay K, Wieringa B et al (2000) Direct evidence for the control of mitochondrial respiration by mitochondrial creatine kinase in oxidative muscle cells in situ. *J Biol Chem* 275:6937–6944
 22. van Deursen J, Wieringa B (1994) Approaching the multifaceted nature of energy metabolism: inactivation of the cytosolic creatine kinases via homologous recombination in mouse embryonic stem cells. *Mol Cell Biochem* 133–134:263–274
 23. Steeghs K, Oerlemans F, de Haan A et al (1998) Cytoarchitectural and metabolic adaptations in muscles with mitochondrial and cytosolic creatine kinase deficiencies. *Mol Cell Biochem* 184:183–194
 24. de Groof AJ, Smeets B, Groot Koerkamp MJ et al (2001) Changes in mRNA expression profile underlie phenotypic adaptations in creatine kinase-deficient muscles. *FEBS Lett* 506:73–78
 25. de Groof AJ, Oerlemans FT, Jost CR et al (2001) Changes in glycolytic network and mitochondrial design in creatine kinase-deficient muscles. *Muscle Nerve* 24:1188–1196
 26. Jost CR, Van Der Zee CE, In 't Zandt HJ et al (2002) Creatine kinase B-driven energy transfer in the brain is important for habituation and spatial learning behaviour, mossy fibre field size and determination of seizure susceptibility. *Eur J Neurosci* 15:1692–1706
 27. In 't Zandt HJ, Renema WK, Streijger F et al (2004) Cerebral creatine kinase deficiency influences metabolite levels and morphology in the mouse brain: a quantitative in vivo ¹H and ³¹P magnetic resonance study. *J Neurochem* 90:1321–1330
 28. Momken I, Lechene P, Koulmann N et al (2005) Impaired voluntary running capacity of creatine kinase-deficient mice. *J Physiol* 565:951–964
 29. Streijger F, Oerlemans F, Ellenbroek BA et al (2005) Structural and behavioural consequences of double deficiency for creatine kinases BCK and UbCKmit. *Behav Brain Res* 157:219–234
 30. Novotova M, Pavlovicova M, Veksler VI et al (2006) Ultrastructural remodeling of fast skeletal muscle fibers induced by invalidation of creatine kinase. *Am J Physiol Cell Physiol* 291:C1279–C1285
 31. Spindler M, Meyer K, Stromer H et al (2004) Creatine kinase-deficient hearts exhibit increased susceptibility to ischemia-reperfusion injury and impaired calcium homeostasis. *Am J Physiol Heart Circ Physiol* 287:H1039–H1045
 32. Speer O, Back N, Buerklen T et al (2005) Octameric mitochondrial creatine kinase induces and stabilizes contact sites between the inner and outer membrane. *Biochem J* 385:445–450
 33. Ito S, Karnovsky JM (1968) Formaldehyde-glutaraldehyde-trinitrofixation (Yellow fix). *J Cell Biol* 39:168a–169a
 34. Dzeja PP, Terzic A (2003) Phosphotransfer networks and cellular energetics. *J Exp Biol* 206:2039–2047
 35. Miller EE, Evans AE, Cohn M (1993) Inhibition of rate of tumor growth by creatine and cyclocreatine. *Proc Natl Acad Sci USA* 90:3304–3308
 36. O'Gorman E, Beutner G, Dolder M et al (1997) The role of creatine kinase in inhibition of mitochondrial permeability transition. *FEBS Lett* 414:253–257
 37. Kroemer G, Galluzzi L, Brenner C (2007) Mitochondrial membrane permeabilization in cell death. *Physiol Rev* 87:99–163
 38. Wallimann T, Dolder M, Schlattner U et al (1998) Some new aspects of creatine kinase (CK): compartmentation, structure, function and regulation for cellular and mitochondrial bioenergetics and physiology. *Biofactors* 8:229–234
 39. Kreider RB (2003) Effects of creatine supplementation on performance and training adaptations. *Mol Cell Biochem* 244:89–94
 40. Brosnan JT, Brosnan ME (2007) Creatine: endogenous metabolite, dietary, and therapeutic supplement. *Annu Rev Nutr* [Epub ahead of print]
 41. Balsom PD, Soderlund K, Ekholm B (1994) Creatine in humans with special reference to creatine supplementation. *Sports Med* 18:268–280
 42. Wyss M, Wallimann T (1994) Creatine metabolism and the consequences of creatine depletion in muscle. *Mol Cell Biochem* 133–134:51–66
 43. Guerrero-Ontiveros ML, Wallimann T (1998) Creatine supplementation in health and disease. Effects of chronic creatine ingestion in vivo: down-regulation of the expression of creatine transporter isoforms in skeletal muscle. *Mol Cell Biochem* 184:427–437
 44. Beal MF (2003) Bioenergetic approaches for neuroprotection in Parkinson's disease. *Ann Neurol* 53 Suppl 3:S39–S47; discussion S47–8
 45. Andres RH, Ducray AD, Huber AW et al (2005) Effects of creatine treatment on survival and differentiation of GABA-ergic neurons in cultured striatal tissue. *J Neurochem* 95(1):33–45
 46. Andres RH, Huber AW, Schlattner U et al (2005) Effects of creatine treatment on the survival of dopaminergic neurons in cultured fetal ventral mesencephalic tissue. *Neuroscience* 133:701–713
 47. Hausmann ON, Fouad K, Wallimann T, et al (2002) Protective effects of oral creatine supplementation on spinal cord injury in rats. *Spinal Cord* 40:449–456
 48. Berneburg M, Gremmel T, Kurten V et al (2005) Creatine supplementation normalizes mutagenesis of mitochondrial DNA as well as functional consequences. *J Invest Dermatol* 125:213–220
 49. Zemtsov A (2007) Skin phosphocreatine. *Skin Res Technol* 13:115–118